



Loss of Tenascin-X expression during tumor progression: A new pan-cancer marker



Sophie Liot^a, Alexandre Aubert^a, Valérie Hervieu^b, Naïma El Kholti^a, Joost Schalkwijk^c, Bernard Verrier^a, Ulrich Valcourt^a and Elise Lambert^a

a - Laboratoire de Biologie Tissulaire et Ingénierie Thérapeutique (LBTI), UMR CNRS 5305, Université Lyon 1, Institut de Biologie et Chimie des Protéines, 7, passage du Vercors, F-69367 Lyon Cedex 07, France

b - Service d'Anatomopathologie, Groupement Hospitalier Est, Hospices Civils de Lyon, Lyon, France

c - Radboud Institute for Molecular Life Sciences, Faculty of Medical Sciences, 370 Geert Grooteplein-Zuid 26 28, 6525 GA Nijmegen, Netherlands

Correspondence to Ulrich Valcourt and Elise Lambert: ulrich.valcourt@ibcp.fr, elise.lambert@ibcp.fr
<https://doi.org/10.1016/j.mbplus.2020.100021>

Abstract

Cancer is a systemic disease involving multiple components produced from both tumor cells themselves and surrounding stromal cells. The pro- or anti-tumoral role of the stroma is still under debate. Indeed, it has long been considered the main physical barrier to the diffusion of chemotherapy by its dense and fibrous nature and its poor vascularization. However, in murine models, the depletion of fibroblasts, the main ExtraCellular Matrix (ECM)-producing cells, led to more aggressive tumors even though they were more susceptible to anti-angiogenic and immuno-modulators. Tenascin-C (TNC) is a multifunctional matricellular glycoprotein (*i.e.* an ECM protein also able to induce signaling pathway) and is considered as a marker of tumor expansion and metastasis. However, the status of other tenascin (TN) family members and particularly Tenascin-X (TNX) has been far less studied during this pathological process and is still controversial. Herein, through (1) *in silico* analyses of the Gene Expression Omnibus (GEO) and The Cancer Genome Atlas (TCGA) databases and (2) immunohistochemistry staining of Tissue MicroArrays (TMA), we performed a large and extensive study of TNX expression at both mRNA and protein levels (1) in the 6 cancers with the highest incidence and mortality in the world (*i.e.* lung, breast, colorectal, prostate, stomach and liver) and (2) in the cancers for which sparse data regarding TNX expression already exist in the literature. We thus demonstrated that, in most cancers, TNX expression is significantly downregulated during cancer progression and we also highlighted, when data were available, that high *TNXB* mRNA expression in cancer is correlated with a good survival prognosis.

© 2020 The Authors. Published by Elsevier B.V. This is an open access article under the CC BY-NC-ND license (<http://creativecommons.org/licenses/by-nc-nd/4.0/>).

Introduction

A normal tissue stroma is essential for the maintenance and the integrity of epithelial tissues and contains a multitude of cells (fibroblasts, immune and endothelial cells) that collaborate to sustain normal tissue homeostasis through direct cell-cell contacts, cell-ECM interactions or cytokine and matrikine release [1,2].

Tumor development is a multi-step process initially involving (1) chronic inflammation and viral and bacterial infections [3] and/or (2) the genetic alter-

ation of critical genes thus allowing the selection of the malignant cells with the highest proliferative potential [4]. The newly formed primary tumor then educates its surrounding environment thanks to (1) secretion of a broad range of cancer-derived factors and (2) specific stimuli, such as local hypoxia and oxidative stress, which thus enable the evolution of normal surrounding stroma into a Tumor MicroEnvironment (TME). This TME basically consists of (1) the nonmalignant cells of the tumor, such as Cancer-Associated Fibroblasts (CAFs), specialized mesenchymal cell types distinctive to each tissue

environment, innate and adaptive immune cells and vasculature with endothelial cells and pericytes and (2) a modified ECM [5–7]. During cancer progression, stroma thus dramatically evolves thanks to the proliferation of CAFs and the subsequent deposition of a dense ECM displaying a particular composition. This process, common to most carcinomas and known as desmoplastic reaction, allows the establishment of “the soil” favorable to tumor cell (“seed”) proliferation, invasion and metastasis [8–13].

Over the past decade, intense progress has been made on the knowledge of the TME and the tumor-stroma crosstalk and leads us to consider new prognostic tools or new therapeutic strategies aiming at a disruption of the dynamics of tumor-stroma interactions. One of the most promising strategies is to specifically target the CAFs of the TME. However, this approach is still in progress and faces different barriers in cancer mouse models and in clinical trials such as CAFs heterogeneity, multiple and sometimes opposite functions of the different CAF subpopulations, diversity of responses in the various studied carcinomas. Altogether, these issues thus underline the absolute requirement for a more in-depth and accurate knowledge of TME composition, function and evolution during cancer progression [14].

Normal ECM is a non-cellular three-dimensional macromolecular network composed of collagens, proteoglycans/glycosaminoglycans, elastin, fibronectin, laminins, and several other glycoproteins. This ECM is a highly dynamic structural network that continuously undergoes remodeling during normal and pathological conditions [15,16]. In the tumor context, various ECM proteins are particularly involved, notably (1) the Matrix Metalloproteinases (MMPs) and Lysyl-Oxidase family members, which are able to degrade and remodel the pre-existing ECM and to initiate crosslinking of the newly synthesized matrix components and (2) the matricellular proteins, for their role as cell signaling initiator [17,18]. Among the matricellular proteins, Tenascin-C has been largely reported to be associated with cancer [19,20].

In mammals, the Tenascin (TN) family includes four members, called TNC, TNR, TNW, and TNX, all of them sharing a common molecular architecture: a N-terminal region that enables trimerization through coiled-coil interactions, followed by epidermal growth factor-like repeats, a series of fibronectin type III (FNIII) modules and a fibrinogen (FBG)-related domain at the C-terminal end. While TNX and TNR form tribrachions, TNC and TNW form hexabrachions thanks to N-terminal cysteines that can support the covalent linking of two trimers [21].

Each TN displays a unique spatio-temporal expression pattern. TNC, the first and the best described member of Tenascins, is widely expressed in the embryo at sites of epithelial-

mesenchymal interactions and around motile cells, including neural crest cells, migrating neuroblasts and glial precursors. It is also found at sites of branching morphogenesis and in developing smooth muscle, bone and cartilage. In the adult, TNC expression is restricted to few tissues exhibiting high tensile stress and in some stem cell niches [22,23]. However, TNC is known to be *de novo* expressed during pathological processes and is now considered as a classic marker of tumor progression [24]. Furthermore, its re-expression is correlated with poor prognosis in melanoma, colorectal, breast, oesophageal, prostate and gastric cancers [17,25–30]. In mammalian embryos, TNW is primarily expressed at sites of osteogenesis, whereas in adults, TNW is completely absent except in certain stem cell niches [31]. Interestingly, analyses of human biopsies revealed a prominent *de novo* expression in all tumors investigated. TNW is thus overexpressed in the tumor stroma of breast, colorectal, brain (oligodendroglioma, astrocytoma and glioblastoma), kidney (clear cell carcinoma, papillary carcinoma, chromophobe renal carcinoma, and oncocytoma), ovarian, prostate, pancreas, and lung cancers as well as in melanomas [31–35]. TNR expression pattern is almost exclusively located to the central nervous system but transiently appears also in Schwann cells during peripheral nerve development [36–40]. TNR is overexpressed in specific brain cancers, *i.e.* in pilocytic astrocytoma, oligodendroglioma and ganglioglioma, but not glioblastoma, suggesting that it could act as a suppressor of glioma invasion [41,42].

TNX protein, encoded by the *TNXB* gene, is ubiquitously expressed in the late, but not in the early, stages of embryonic development indicating that this glycoprotein is mainly involved in organogenesis [20,43,44]. In adult, TNX is ubiquitously expressed in connective tissues of a large variety of organs, where it has been shown to play a crucial role in the collagenous network assembly and organization [20,45]. Compared to the other tenascins, the status of TNX expression during cancer progression has been far less studied and is relatively controversial. Indeed, TNX expression has been described to be downregulated in the stroma of tumors formed following renal carcinoma cell transplantation [46], but also in high-grade astrocytomas [47], Malignant Peripheral Nerve Sheath Tumors (MPNST) [48], melanoma [49] and leiomyoma [50], but was shown to be up-regulated in malignant mesothelioma [51–53] and ovarian cancer [54].

Herein, we thus decided to perform a large meta-analysis to evaluate TNX expression during tumor progression and chose to focus on the 6 cancers with the highest incidence and mortality in the world, *i.e.* lung, breast, colorectal, prostate, stomach and liver carcinoma (Table 1 - Globocan 2018 - <http://>

Table 1. New cases and deaths for the selected cancers in 2018

Cancer site	New Cases		Deaths	
	Rank	No. of cases (% of all sites)	Rank	No. of cases (% of all sites)
Lung	1	2,093,876 (11.6)	1	1,761,007 (18.4)
Breast	2	2,088,849 (11.6)	4	626,679 (6.6)
Prostate	3	1,276,106 (7.1)	8	358,989 (3.8)
Colon	4	1,096,601 (6.1)	5	551,269 (5.8)
Stomach	5	1,033,701 (5.7)	2	782,685 (8.2)
Liver	6	841,080 (4.7)	3	781,631 (8.2)
Kidney	15	403,262 (2.2)	17	175,098 (1.8)
Brain, Nervous System	18	296,851 (1.6)	13	241,037 (2.5)
Ovary	19	295,414 (1.6)	15	184,799 (1.9)
Skin (melanoma)	20	287,723 (1.6)	24	60,712 (0.6)
Mesothelium (pleura)	34	30,443 (0.2)	29	25,576 (0.3)

gco.iarc.fr). Additionally, we included in our meta-analysis the 7 specific types of cancer already described in the literature to further validate our study and clarify previously published data performed with a low number of samples or restrictive datasets. We thus analyzed *TNX* expression in 13 types of cancer compared to normal equivalent tissues at the mRNA and protein levels (Table 1). *TNXB* mRNA expression was evaluated (1) by dissecting 90 GSE datasets from the Gene Expression Omnibus (GEO) database and (2) by using the UALCAN interactive web-portal to perform in-depth analyses of TCGA gene expression data [55]. In parallel, *TNX* expression was evaluated at the protein level on a pan-cancer Tissue MicroArray by immunohistochemistry followed by a quantitative imaging analysis and a blind scoring by an anatomopathologist.

Collectively, our results demonstrated (1) *TNX* is downregulated in most cancers, except gliomas, and (2) high *TNXB* mRNA expression in tumoral samples is correlated with a good survival prognosis in the 2 cancers with the highest incidence and mortality worldwide, *i.e.* breast and lung carcinomas, thus demonstrating that *TNX* could be used as a new diagnosis and prognosis marker of cancer.

Results

TNXB mRNA expression is mainly downregulated during carcinogenesis

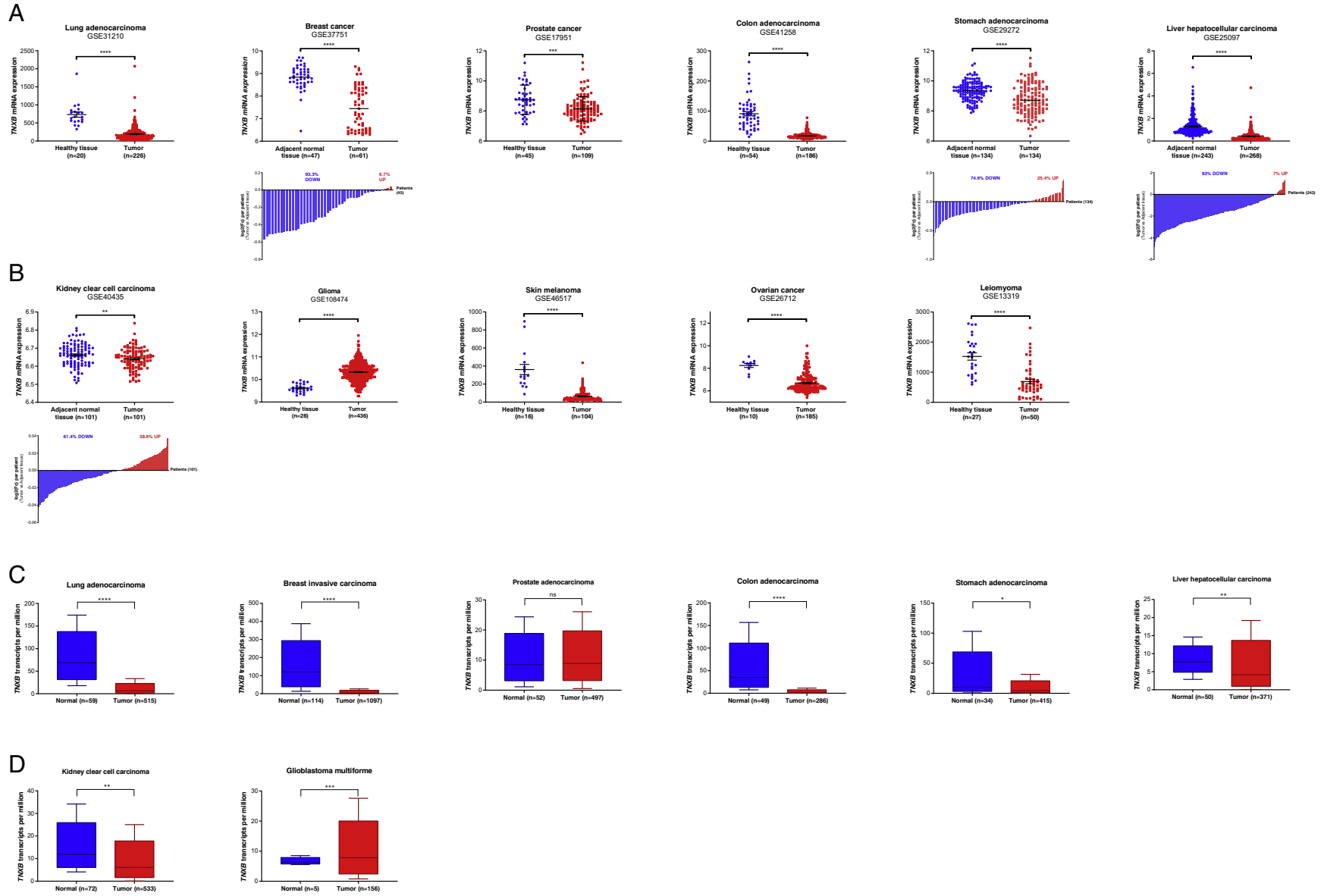
The aim of our study was to determine whether *TNX* mRNA and protein levels were significantly dysregulated in various cancer types compared to normal tissues (Table 1). For gene expression analysis, we focused on two databases: (1) The Gene Expression Omnibus (GEO) database, which is a public functional genomics data repository, and (2) The Cancer Genome Atlas (TCGA), this latter being analyzed through UALCAN, an integrated data-mining platform to harness the potential of

cancer transcriptome [55]. For the GEO database analyses, we performed a pre-screening of all the published datasets and only listed the most recent ones (from 2009) by excluding the datasets without healthy controls. To avoid interpatient variability, when possible, we chose the datasets with adjacent control tissues except for the prostate carcinoma, for which it is clearly established that the gene expression pattern in tissues adjacent to prostate cancer is so substantially altered that it resembles a cancer field effect [56]. For malignant mesothelioma, we only focused on malignant pleural mesothelioma, since this specific neoplasia (1) accounts for 80–90% of all diagnosed cases and (2) was the subject of a previously published study [53]. Furthermore, we only selected the datasets with pleura as normal samples to perform a proper comparison between normal and tumoral tissues. Finally, for dataset selection, we excluded datasets with low number of samples (<20 normal or tumoral cases) except for rare carcinomas, for which datasets with high number of normal samples were not available, *i.e.* MPNST, skin melanoma, ovarian cancer and malignant mesothelioma (Supplementary data S1).

Therefore, we investigated 90 GSE datasets for the 13 selected types of cancer (Table 1) and an overall analysis showed *TNXB* gene was

Table 2. Summary of the analyzed G.E.O datasets.

Cancer site	Nb of datasets	Variation		
		DOWN	UP	ns
Lung	13	11	0	2
Breast	7	7	0	0
Prostate	2	2	0	0
Colon	15	11	1	3
Stomach	14	9	0	5
Liver	10	6	0	4
Kidney	7	6	0	1
Cerebrum (glioma)	2	0	2	0
Ovary	10	9	0	1
Skin (melanoma)	3	3	0	0
Uterus (leiomyoma)	2	2	0	0
Pleura (mesothelium)	3	1	0	2
Peripheral nerve sheath	2	0	0	2
TOTAL	90	67	3	20
% of datasets		74.44	3.33	22.22



significantly downregulated for 67 of them (74.4%), upregulated for 3 of them (3.3%) and not significantly altered in 20 of them (22.2%) (Table 2 and Supplementary data S1). For each cancer, we next analyzed the pre-screened datasets and evaluated the number of datasets for which *TNXB* mRNA expression was significantly up- or down-regulated. We then established the regulation trend for *TNXB* mRNA expression and chose the most representative dataset for each cancer with the highest number of samples by selecting the dataset with clinical data when available (Supplementary data S1). In all the selected cancers with the highest incidence and mortality worldwide, we thus clearly observed a significant downregulation of *TNXB* gene expression. Indeed, compared to normal tissues, we found a 78.5% decrease of *TNXB* mRNA expression in lung cancer, 15.8% in breast, 7.2% in prostate, 81.2% in colorectal, 6.8% in gastric and 71.4% in liver carcinomas (Fig. 1A). *TNXB* gene expression was also significantly downregulated in kidney clear cell carcinoma (−0.30%) and leiomyoma (−63.4%) (Fig. 1B). For skin melanoma and ovarian cancer, we also concluded that *TNXB* mRNA expression was downregulated during cancer progression of 85.6% and 23.8% respectively, even if the initial fixed cut-off of 20 control or tumoral samples was not reached (Fig. 1B). We could not conclude regarding the status of *TNXB* gene expression in MPNST and malignant mesothelioma due to the very low number of normal tissue samples (≤ 5 samples) (Supplementary data S1 – MPNST and Malignant Mesothelioma). Finally, *TNXB* expression was unexpectedly upregulated by 7.5% in glioma compared to healthy controls (Fig. 1B). As mentioned previously, when available, we selected datasets with adjacent normal tissues as controls to exclude inter-individual variability. We were thus able to demonstrate a downregulation of *TNXB* mRNA expression in tumoral sample compared to adjacent normal tissue for patients suffering of breast cancer (in 93.3% of analyzed patients), stomach adenocarcinoma (74.6%), liver hepatocellular carcinoma (93%) and kidney clear cell carcinoma (61.4%) (Fig. 1A and B, lower bar charts). For datasets for which clinical information were available, we have also analyzed more precisely *TNXB* expression status in various clinical subgroups referring to (1) classical mutation

status (ALK fusion, EGFR and KRAS mutations) or the Myc oncogene expression status in lung adenocarcinoma, (2) the breast cancer subtypes (Estrogen Receptor positive or negative carcinoma; Triple negative carcinoma or other subtypes), (3) p53 mutation status in colon adenocarcinoma or to (4) the various subtypes of glioma (astrocytoma, glioblastoma multiforme and oligodendroglioma) (Supplementary Fig. S2A). We thus demonstrated that *TNXB* expression was downregulated in all subgroups of lung, breast and colon carcinomas compared to the group composed of equivalent healthy tissues and we definitively showed that *TNXB* mRNA level was upregulated in all glioma subtypes compared to equivalent normal samples (Supplementary Fig. S2A).

To validate our results obtained through GEO database analyses, we also studied The Cancer Genome Atlas database through the UALCAN web-portal [55]. TCGA only focuses on 33 selected types of cancer, explaining why information were absent for leiomyoma and MPNST. Additionally, we could not conclude for ovarian carcinoma, malignant mesothelioma and skin melanoma because, in TCGA database, no or only one normal sample was available. However, this database allowed us to show that *TNXB* mRNA expression was downregulated in lung (−89.9%), breast (−96.4%), colon (−94.8%), stomach (−56.1%), liver (−46%) and renal (−48.7%) carcinomas (Fig. 1C and D), thus confirming the results obtained from the GEO database. Nevertheless, *TNXB* mRNA level was not significantly regulated in prostate adenocarcinoma compared to normal tissue (Fig. 1C). Once again, *TNXB* expression was upregulated (+21.3%) in glioblastoma multiforme compared to normal samples (Fig. 1D), in contrast to previously published data [47]. Altogether, this extensive *in silico* analysis enabled us to demonstrate that *TNXB* expression was downregulated in most analyzed cancers except in brain tumors where it was upregulated.

***TNXB* downregulation in cancer is confirmed at the protein level**

We next studied *TNX* protein level through analysis of a pan-cancer TMA following

Fig. 1. Variation of *TNXB* mRNA expression in tumors versus normal or adjacent tissues. Cancers of high incidence/mortality were studied (A and C), as well as cancers for which *TNX* status had been previously studied (B and D). A and B: Expression values of *TNXB* mRNA obtained from the selected datasets extracted from the GEO database. Non-parametric paired (breast, stomach, liver, and kidney cancers) and unpaired (lung, prostate, colon, glioma, ovary, melanoma and leiomyoma cancers) tests were performed comparing tumoral to normal tissues. For datasets comparing *TNXB* mRNA expression in tumoral sample versus adjacent normal tissue, a bar chart is presented just below the first graphical representation. Each bar corresponds to a patient and is either blue, when *TNXB* mRNA expression is downregulated in tumoral sample or red, when *TNXB* expression is upregulated. C and D: Expression data and associated p-values extracted from the UALCAN web-portal. Numbers of tumoral and control samples for each dataset are indicated. ***p < 0.0001; **p < 0.001; *p < 0.01 and *p < 0.05.

immunohistochemistry and quantitative staining analysis or through blind scoring by an anatomopathologist. This pan-cancer array comprised at least 8 healthy tissues and 20 tumoral samples for each type of analyzed cancers, except for malignant mesothelioma. For this specific cancer, we used a malignant mesothelioma Tissue MicroArray, which was the only commercial array available with equivalent healthy tissue samples. Prior to the experiment, four different TNX antibodies raised against the C-terminal region of the human TNX were assessed on human skin sections: two commercially available (sc-271594, clone F11, from Santa Cruz and AF6999 from R&D systems) and two home-made antibodies (kindly provided by Joost SCHALKWIJK and Manuel KOCH) (Supplementary Fig. S3A). All antibodies, except the one from R&D systems, showed a similar and specific staining of TNX in the dermis of healthy donors, as expected [57] (Supplementary Fig. S3B). We selected the clone F11 from Santa Cruz (sc-271594), which (1) demonstrated the strongest staining in the dermis of healthy donor with no background in the epidermis (Supplementary Fig. S3B) and (2) led to no staining on skin sections of patient suffering of classical-like Ehlers-Danlos syndrome (EDS due to TNX deficiency) (Supplementary Fig. S3C). This mouse monoclonal antibody is specific for a short epitope (14 amino-acids) mapping the fibrinogen-related domain at the C-terminus of human TNX and does not cross-react with the FBG domain of other TN family members (data not shown).

As expected, TNX was immunodetected in the ECM of normal samples. A stroma-specific quantification of TNX labelling using Fiji software was performed (Supplementary Fig. S4). In order to overcome the histological heterogeneity of cancers and origin of tissues, we repeated the segmentation training for each tissue spot. We thus demonstrated that TNX protein level was significantly decreased in the stroma of lung, breast, prostate, colon, liver, kidney and uterus carcinomas as well as in skin melanoma, compared to equivalent normal tissues (Fig. 2A and B). The downregulation was not significant for ovary carcinoma due to 3 highly positive tumor samples, whereas the others were definitely negative for TNX labelling (Fig. 2A and B and Supplementary Fig. S5). For malignant pleura mesothelioma, a decrease in TNX level was also observed, however statistical analysis could not be performed due to the very low number of samples available. For stomach adenocarcinoma, a non-significant upregulation was observed compared to equivalent normal samples, which was at odds with the results obtained through the GEO and TCGA database analyses. Furthermore, and as already deduced through GEO and TCGA database analyses, TNX protein level was significantly upregulated in gliomas compared to equivalent healthy samples

(Fig. 2A and B). Finally, we confirmed that TNX protein level in tumoral samples was observed regardless of the subtype of analyzed cancer (Supplementary Fig. S2B). All tissue core quantifications were confirmed through blind scoring by a clinical anatomopathologist (Fig. 2C), thus definitely demonstrating that TNX protein level is markedly diminished in most of the analyzed cancers.

TNXB mRNA expression is correlated with tumor progression and should be considered as a new prognosis marker in cancer

As mentioned above, for the GEO dataset selection, we chose, when available, datasets associated with clinical data, *i.e.* grade/stage and survival. We first studied *TNXB* expression levels in the various clinical stages or grades of cancer development. Therefore, we demonstrated that the decrease in *TNXB* expression observed in lung and breast carcinomas is all the more important that the stage of tumor development is advanced (Fig. 3A and B). Inversely, *TNXB* expression levels increased concomitantly with the grade of glioma (Fig. 3C).

Datasets for lung and breast carcinomas also presented clinical survival information. We thus analyzed the expression of *TNXB* mRNA in tumoral samples and established *TNXB*^{low} and *TNXB*^{high} expression subgroups by median cut-off on *TNXB* expression values, meaning that the 50% of patients with lowest expression values were considered as "*TNXB*^{low}" and the 50% of patients with highest expression values were considered as "*TNXB*^{high}". Therefore, we demonstrated that the percentage of patient survival is significantly higher in *TNXB*^{high} subgroups compared to *TNXB*^{low} subgroups for lung adenocarcinoma ($p = 0.0014$, Fig. 3D) and for breast carcinoma ($p = 0.0234$, Fig. 3E).

Altogether, these data clearly demonstrated that *TNXB* expression is correlated with tumor progression and that high level of *TNXB* mRNA is a good survival marker in carcinomas and could thus be used as a novel survival prognosis marker.

Discussion

Through *in silico* analysis of expression data and immunohistological approaches, we demonstrated TNX mRNA and protein levels are downregulated in most cancers, except for glioma where TNX expression is upregulated (Table 3). In this study, we only focused on the 6 cancers with the highest incidence and mortality worldwide and the 7 cancers already described for TNX expression. However, the pan-cancer TMA we immunostained also contained other types of cancer (such as bladder, uterus, head and neck carcinomas) and a simple microscopic observation of the TNX staining enabled us to confirm that our results

can be generalized to most cancers (Supplementary Fig. S5), suggesting that TNX is a good pan-cancer marker. Furthermore, we performed equivalent *in silico* analyses focusing on *TNC* and *TNW* genes and we definitely confirmed that TNX presented a particular interest as prognosis and diagnosis marker among TN family (Supplementary Figs. S6 and S7). This discovery could be of great importance since even MMPs that are known to be regulated during tumor progression can hardly be considered as pan-

cancer markers [58]. Our results are reinforced by the data recently published by Chakravarthy et al., in which they examined TCGA database and analyzed the pan-cancer landscape of ECM gene dysregulation in 8043 malignant tissues from 15 different tumor types and 704 corresponding normal tissues. In this study, 58 out of the 249 ECM genes represented in the RNA-seq dataset were significantly dysregulated; 30 of them were upregulated and 28 of them were downregulated. Interestingly,

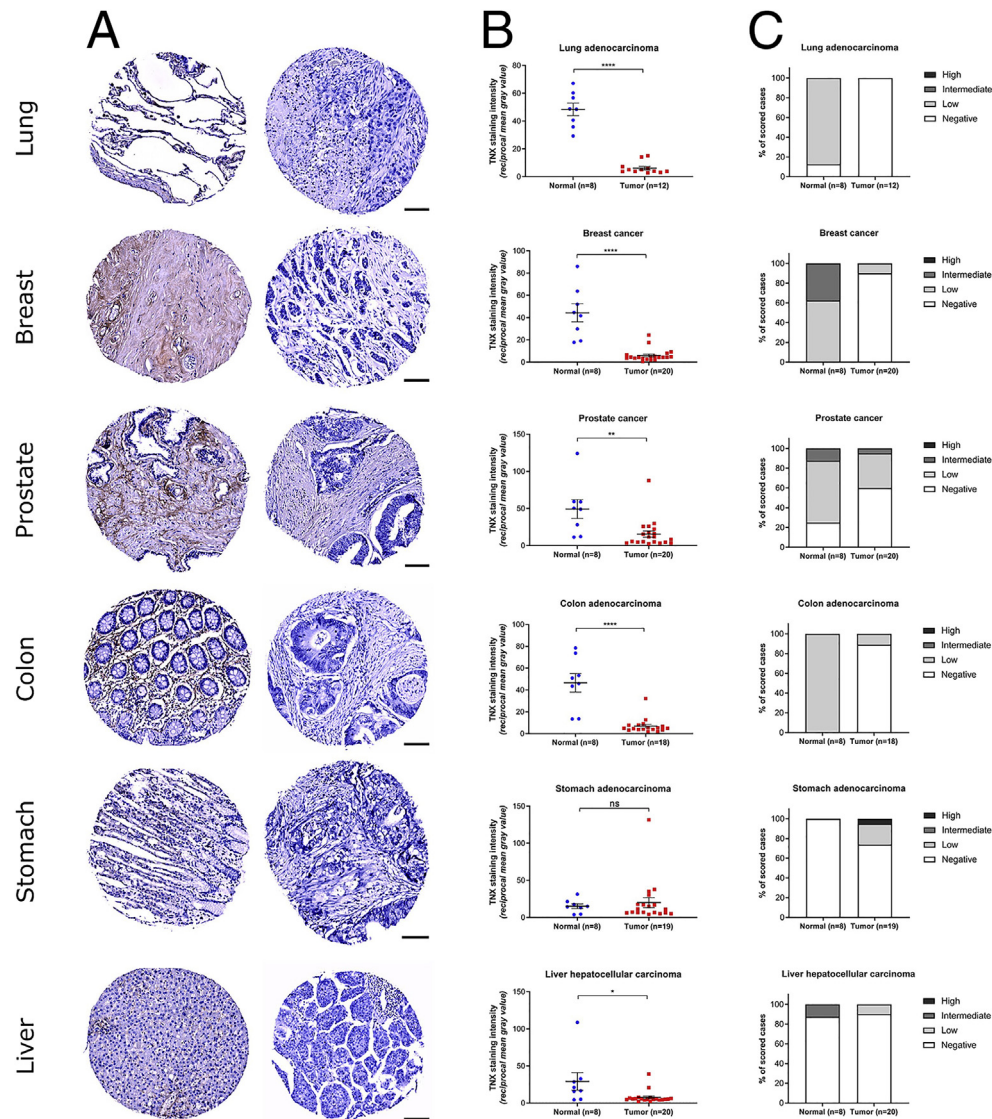


Fig. 2. TNX protein level in tumoral versus normal tissues. Cancers of high incidence/mortality were studied (upper part), as well as cancers for which TNX status was previously studied (lower part) thanks to TNX immunolabelling of tissue sections on Tissue MicroArray slides (#MC6163 and #T392a). A: Representative cores of normal (left) and tumoral (right) tissues. Scale bar = 100 μ m. B: Quantification of stromal TNX staining intensity. A segmentation between stromal and epithelial areas was performed, followed by measurement of reciprocal mean grey value (staining intensity) in the stromal area. Segmentation training was newly performed for each spot. Mann-Whitney test was performed between normal and tumoral conditions (**** $p < 0.0001$; *** $p < 0.001$; ** $p < 0.01$ and * $p < 0.05$). C: Clinical sample scoring. Staining was blindly scored according to 4 categories: negative, low, intermediate and high. Results are presented as percentage of total cores for each cancer type.

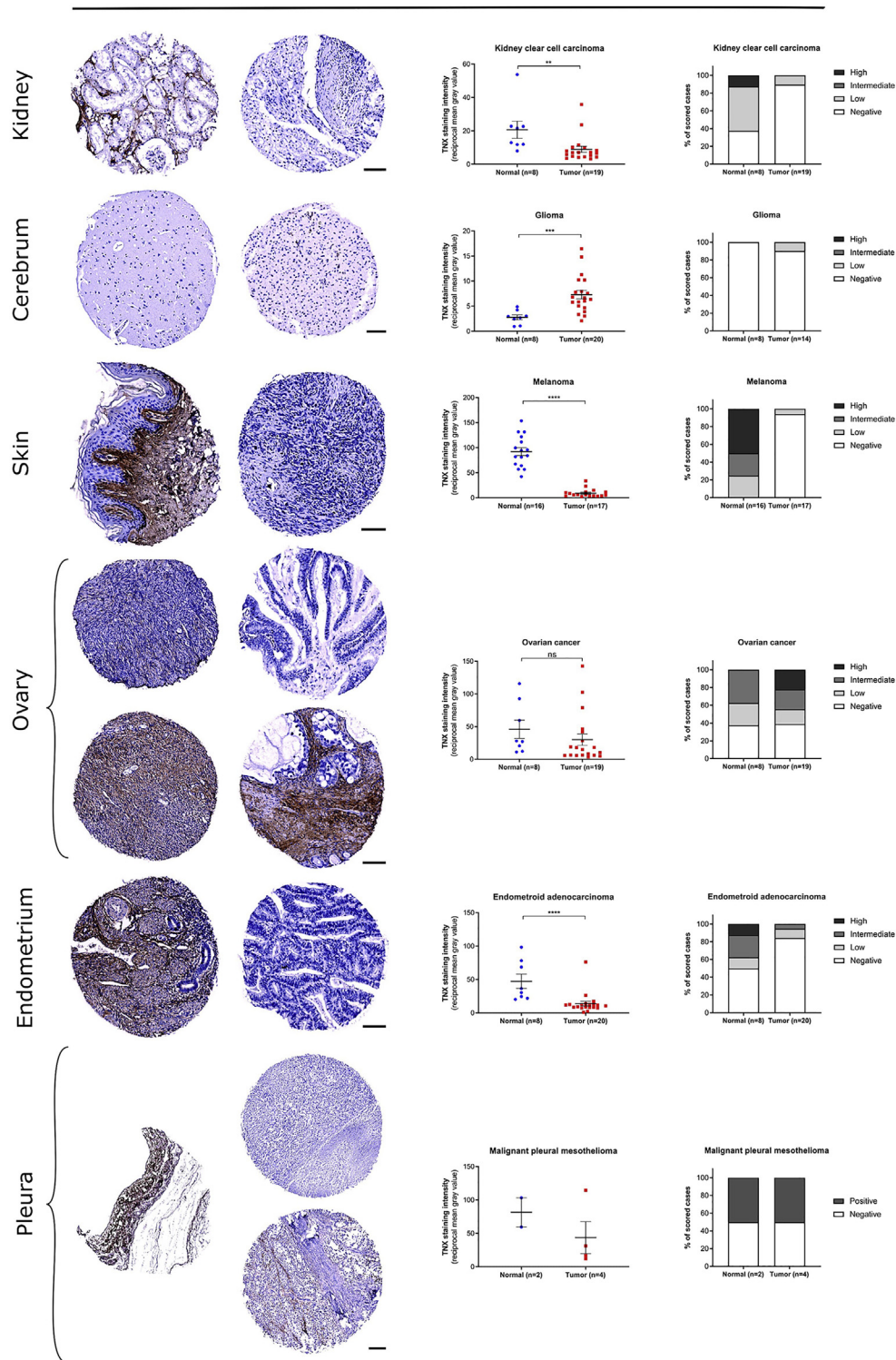


Fig. 2. (continued).

the gene which was the most significantly downregulated in cancers, was *TNXB* [59].

Obviously, this large study also leads to many questions and notably regarding the relevance of

TNX regulation in all subtypes of cancers but we demonstrate when data were available that, except for gliomas in which TNX was inversely regulated, all subtypes of analyzed cancers presented a *TNXB*

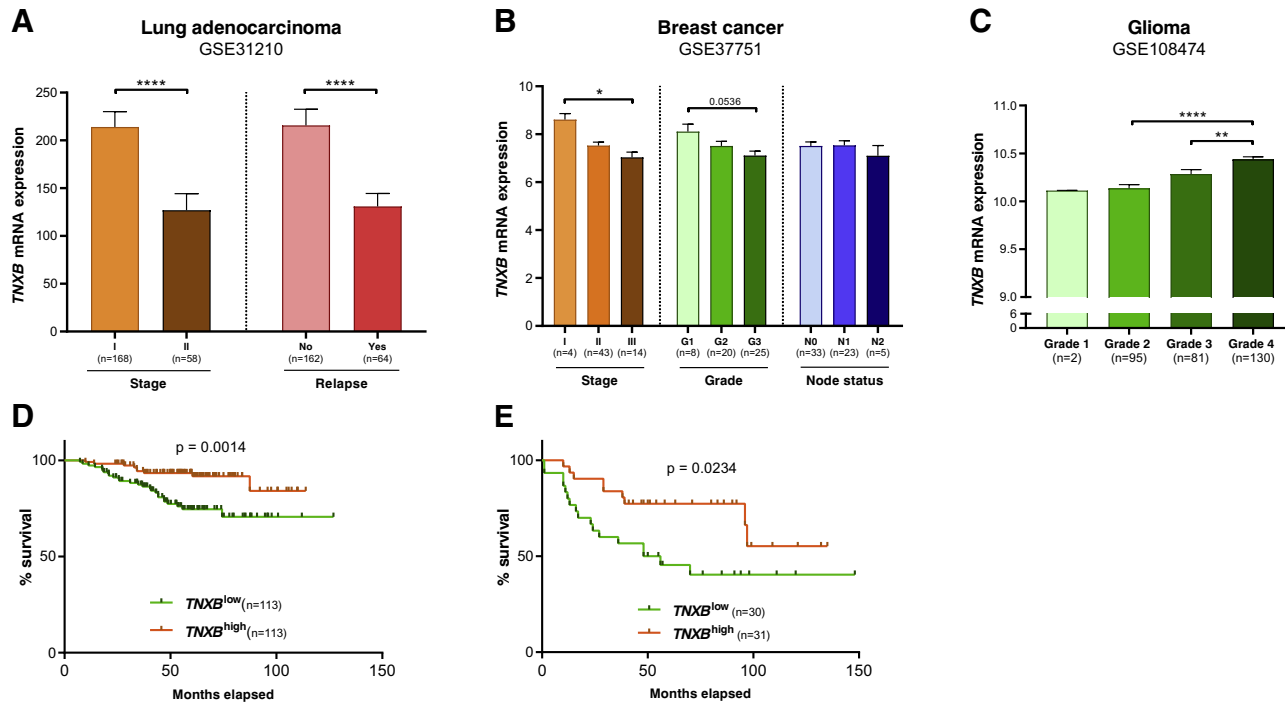


Fig. 3. Prognosis according to *TNXB* expression level in tumors. *TNXB* mRNA levels at various stages or grades of tumor progression in lung adenocarcinoma (A), breast cancer (B) and glioma (C). Comparison of survival probability of patients with *TNXB*^{low} versus *TNXB*^{high} mRNA expression in lung (D) and breast (E) tumors by Kaplan–Meier method. Groups were delimited by median cut-off according to *TNXB* expression values in tumoral samples.

Table 3. Outcomes of the study.

Cancer type	Literature	Bioinformatics analyses		Tissue MicroArray analysis	
		G.E.O. results	UALCAN results	TMA quantification	Clinical scoring
Lung adenocarcinoma	[Grey box]	[Green]	[Green]	[Green]	[Green]
Breast cancer		[Green]	[Green]	[Green]	[Green]
Prostate cancer		[Green]	[White]	[Green]	[Light Green]
Colon adenocarcinoma		[Green]	[Green]	[Green]	[Green]
Stomach adenocarcinoma		[Green]	[Green]	[Green]	[Pink]
Liver hepatocellular carcinoma		[Green]	[Green]	[Green]	[Green]
Kidney clear cell carcinoma	[Green]	[Green]	[Green]	[Green]	[Green]
Glioma	[Green]	[Red]	[Red]	[Red]	[Red]
Ovarian cancer	[Red]	[Green]	[Grey]	[White]	[Pink]
Melanoma of skin	[Green]	[Green]	[Grey]	[Green]	[Green]
Leiomyoma	[Green]	[Green]	[Green]	[Green]	[Green]
Malignant mesothelioma	[Red]	[White]	[Grey]	[Grey]	[Grey]
Malignant Peripheral Nerve Sheath Tumor	[Green]	[White]	[Grey]	[Grey]	[Grey]

Down regulation

Down regulation tendency

Up regulation

Up regulation tendency

Non significant

No data available

repression (Supplementary Fig. S2). However, a fine analysis of *TNX* expression in all subtypes of all cancers has to be realized.

Moreover, whereas the downregulation of *TNX* mRNA and protein levels was robustly observed in most cancers, we also noted some discrepancies between gene and protein expressions in our analyses, as well as with results reported in the literature, as discussed hereafter (Table 3). Indeed, when analyzed in detail, we could observe that for the *in silico* analysis of prostate cancer dataset from TCGA using UALCAN webportal, *TNXB* mRNA expression was not significantly regulated. However, as previously described for the prostate carcinoma, the gene expression pattern in tissues adjacent to prostate cancer is so substantially altered that it resembles a neoplastic tissue [56]. And in fact, control tissues for prostate cancer in TCGA dataset included tumor-adjacent tissues which could lead to misinterpretation [60]. Our hypothesis that *TNX* is diminished in prostate cancer is strengthened by the fact that we observed (1) a significant *TNXB* downregulation in prostate carcinoma through the 2 GEO dataset analyzed and (2) a robust decrease of *TNX* immunostaining in 20 tumors compared to 8 normal samples. Additionally, we are particularly confident in the non-tumoral origin of the “normal tissues” in our pan-cancer TMA since they were collected from healthy patients between 30 and 40-year-old and the average age at which prostate cancer is diagnosed is 73-year-old (<http://gco.iarc.fr/>).

For stomach adenocarcinoma, our results showed *TNXB* mRNA expression was significantly downregulated, whereas *TNX* protein detection by immunohistochemistry revealed an upregulation trend even if it was not significant. The stomach is composed of three anatomical regions: (1) the cardiac, which contains mucous secreting glands (called cardiac glands) and is closest to the oesophagus, (2) the fundus (corpus), the body or largest part of the stomach which contains the gastric (fundic) glands and (3) the pyloric, which secretes the gastrin hormone and two types of mucus. Clinicopathological and molecular analyses have evidenced the diversity of gastric carcinoma and led researchers to classify gastric carcinomas in three subgroups according to their location for appropriate management [61]. In the used TMA, localization of tumor and normal samples has not been specified. However, a detailed histological analysis allowed us to conclude that most healthy samples could correspond to the fundus which is known by anatomopathologists to be particularly reactive to unspecific immunostainings (and were scored as negative by our specialist). Thus, our interpretation could be biased by the origin and unspecific immunoreactivity of the samples and we could not conclude for *TNX* protein regulation during stomach adenocarcinoma formation.

In this report, we definitely demonstrated that *TNX* mRNA and protein levels were significantly upregulated in brain cancer. This result is particularly surprising since *TNX* is downregulated in the other analyzed

cancer types. However, we confirmed the significant upregulation of *TNXB* gene in various glioma subtypes (astrocytoma, glioblastoma multiforme and oligodendroglioma). In brain, the ECM is unique both in its composition and functions. Indeed, in contrast to other tissues, the ECM of the central nervous system lacks fibrous proteins under normal conditions and is enriched in glycoproteins and proteoglycans [62]. We can therefore assume that TNX is differently regulated in this particular tissue during pathological context and notably during tumor progression.

Kramer and colleagues have shown, through TNX immunodetection using AF6999 antibody, that TNX was upregulated in ovary cancer [54]. However, in our hands, this antibody gave unspecific results in the epidermis of human skin and still stained the dermis of TNX-deficient patients (Supplementary Fig. S3). Additionally, our GEO dataset analysis demonstrated that 7 over the 8 selected datasets presented a significant downregulation of *TNXB* during ovarian carcinoma and results for the remaining dataset were not significant (Supplementary data S1). Therefore, our analysis of curated datasets is definitely at odds with the published data. Though, it has to be noted that results obtained through TNX immunohistochemistry on TMA were less clearcut. Indeed, TNX protein expression was predominantly downregulated in most ovarian cancers (16 samples) compared to normal tissues (8 samples), whereas it was drastically upregulated in 3 tumoral samples (Fig. 2). Ovarian cancers can be classified in 5 major clinicopathologically distinct entities: endometrioid carcinoma, clear cell carcinoma, mucinous carcinoma, low-grade serous carcinoma and high-grade serous carcinoma [63]. The 3 TNX-overexpressing tumor samples corresponded to mucinous adenocarcinoma (2 positive cores/11 mucinous adenocarcinomas) and high-grade serous carcinoma (1 positive core/9 high grade serous carcinomas), so we could not attribute this sporadic TNX upregulation to a specific ovary cancer subtype. The ovary tumoral tissues present distinct biological and molecular properties (even within the same histological subtype) demonstrating the complexity of the disease [64] and the need for further investigations regarding TNX protein levels in this particular cancer.

Malignant mesothelioma is a rare disease and among the various forms, the pleural mesothelioma develops in the pleura, a thin membrane of cells lining the lungs and the chest wall. TNX has been shown to be highly expressed in malignant mesothelioma compared to other cancers involving the serosal cavities [51,52]. However, in those studies, no healthy tissue has been analyzed. In contrast, in a very recent study, Nayakama and collaborators have demonstrated that *TNXB* gene expression was upregulated in malignant pleural mesothelioma compared to healthy adjacent tissue using the GSE51024 dataset from GEO database. However, in this study normal paired lung parenchyma was

used as control tissue but does not correspond to equivalent healthy tissue to malignant pleural mesothelioma and is therefore in our view hardly comparable [53]. In the GEO database, no dataset was available with sufficient number of equivalent normal tissues. However, we decided to analyze datasets with low number of proper normal tissue (pleura) but could not demonstrate a regulation of *TNXB* expression with certainty.

A very low number of normal and tumoral samples were also present in the MPNST datasets from GEO and no TMA was available for this specific cancer thus unabling us to conclude for this rare disease.

In this report, we demonstrated *TNXB* mRNA and TNX protein levels were concomitantly and significantly downregulated in various types of cancer, which raises the question of the mechanism(s) leading to the downregulation of *TNXB* gene expression in this pathological context. Very few data are currently available regarding *TNXB* gene regulation. Unlike for the other tenascins, there are so far no report indicating that *TNXB* is regulated by growth factors or cytokines. However, like *TNC* and *TNW*, *TNXB* is subjected to negative regulation by glucocorticoids [40,46,65]. Nevertheless, through GSE dataset analysis, we could not find an upregulation of glucocorticoid receptor (*NR3C1*) mRNA level concomitant with *TNXB* mRNA downregulation. Additionally, assuming that during cancer progression, *TNXB* is regulated in an opposite way compared to *TNC*, this hypothesis is ruled out.

In the human genome, *TNXB* transcription can be initiated from 3 different widely separated promoters [66]. However, only one of the 3 promoters was shown to be the main control region for *TNXB* transcription in all tissues tested and its analysis revealed several putative binding sites for Sp1/Sp3 transcription factors. A cluster of 5 sites close to the Transcription Start Sites (TSSs) was proven to be functional and required for driving *TNXB* expression in fibroblasts [40,66,67]. Another promoter and TSS within the *TNXB* gene were described. This promoter was shown to be activated by hypoxia and subsequent histone deacetylase 1 (HDAC1) dissociation from Sp1/HDAC1 complex [68] resulting in a transcript encoding an N-terminally truncated and shorter TNXB (TNXB-S) protein with cytoplasmic localization [69]. However, the physiological significance of hypoxia-induced expression of *TNXB-S* gene has not yet been understood. Hypoxia corresponds to a non-physiological level of oxygen tension, a phenomenon common in a majority of malignant tumors. We could thus hypothesize that under hypoxic conditions the short TNXB (TNXB-S) protein is favoured at the expense of the long form and that HDAC1 is involved in this process. By analyzing the GEO datasets used for *TNXB* mRNA expression (GSE31210 for lung cancer and GSE37751 for breast cancer), we demonstrated that *HDAC1* mRNA expression was significantly upregulated in lung (Fc = 0.401; p =

$1.30 \cdot 10^{-4}$) and breast ($F_c = 0.457$; $p = 4.90 \cdot 10^{-6}$) carcinomas compared to non-tumoral tissues. To definitely validate our hypothesis, it will be important to analyze the level of TNXB-S protein in tumor samples through the specific antibodies raised against the truncated TNXB (anti-h29 and anti-h30 antibodies developed by Endo et al. [69]).

A number of long non-coding RNAs (lncRNAs) have been shown to play significant roles in the pathogenesis of several cancers including colorectal, kidney and breast cancers [70–72]. Through bioinformatics analysis, Yan and colleagues demonstrated that the lncRNA LINC01305 was the most overexpressed lncRNAs in cervical cancer and that *TNXB* was a target gene of LINC01305. Additionally, an upregulation of LINC01305 in cervical cancer cell lines was observed concomitantly with a downregulation of TNX [73]. In the pan-cancer TMA we used, we also detected lower TNX protein levels in cervical cancer samples compared to adjacent normal cervix tissues (Supplementary Fig. S5). The correlation between *LINC01350* and *TNXB* expressions in cervical cancer prompted us to analyze *LINC01350* expression in our selected GSE datasets where *TNXB* was downregulated, but this link could not be generalized to the other analyzed cancers (data not shown). However, we cannot exclude that other lncRNAs could be responsible for *TNXB* downregulation in cancers and this last hypothesis thus requires further investigations.

Very interestingly, Yan and colleagues also demonstrated that *TNXB* overexpression led to (1) MMP2, MMP9 and vimentin downregulations at both mRNA and protein levels and (2) cervical cancer cell line migration and invasion decreases [73]. These results thus suggest that high *TNXB* expression could limit metastasis formation and thus could be a good prognosis factor during cancer progression. Indeed, in our study, we observed that high *TNXB* expression is correlated with a good survival rate in breast and lung carcinomas. The link between the expressions of TNX protein and gelatinases (MMP-2 and -9) and tumor progression has also been largely described by the group of Matsumoto [74–76]. In our study, a significant upregulation of *MMP9* gene was observed concomitantly with *TNXB* downregulation in most analyzed carcinomas (data not shown) thus suggesting that reinducing *TNXB* expression could be a good pan-cancer therapeutic strategy.

Experimental procedures

In silico analyses

Microarray datasets were selected from the NCBI GEO database (<https://www.ncbi.nlm.nih.gov/gds>).

Results were filtered by date and number of samples.

For all datasets, differentially expressed genes (D.E.G.) between cancer and normal tissues were obtained thanks to GEO2R analysis tool which compares both groups using limma (Linear Models for Microarray Analysis) R package (Bayesian statistics). D.E.G. were determined by Benjamini & Hochberg (False discovery rate) adjusted p -value < 0.05 . Then, representative datasets were selected according to the criteria cited in the “Results” section. For those datasets, *TNXB* expression values were extracted from GEO and plotted. Comparisons between tumoral and non-tumoral tissues were performed using non-parametric paired (Mann-Whitney, when non-tumoral samples were adjacent tissues) or unpaired (Wilcoxon, when non-tumoral samples were healthy tissues) statistical tests. TCGA data were analyzed through UALCAN web-portal and results for *TNXB* gene expression were extracted as presented in the website.

To study *TNXB* mRNA expression during tumor progression, patients were separated depending on their tumor stage or grade and the mean *TNXB* expression value of each group was plotted. Groups were then compared using non-parametric one-way ANOVA (Kruskal-Wallis test) followed by Dunn's multiple comparison test.

Finally, patient survival was studied using datasets containing clinical data. Tumor samples were separated in 2 groups (*TNXB^{low}* and *TNXB^{high}*) by median cut-off on the *TNXB* expression values (50% of patients with the lowest values = *TNXB^{low}*, 50% with the highest values = *TNXB^{high}*). Cumulative survival proportions were estimated using the Kaplan–Meier method and *TNXB^{low}* and *TNXB^{high}* groups were compared thanks to Log-Rank (Mantel-Cox) statistical test.

Immunohistochemistry

TNX immunostaining was performed following a classical protocol. Briefly, after deparaffinization and rehydration, epitopes retrieval step was performed in sodium citrate buffer pH 6 for 20 min at 98 °C. Endogenous peroxidases were then quenched by 3% H₂O₂ (v/v) in phosphate Buffered Saline (PBS) and non-specific sites were blocked with 2.5% (v/v) normal horse serum in Tris-buffered saline (TBS). TNX primary antibodies were incubated in blocking solution overnight at 4 °C and biotinylated secondary antibodies were incubated 30 min at room temperature. Revelation was performed using ABC Reagent and 3,3'-Diaminobenzidine (DAB) chromogen (R.T.U. Vectastain Universal Elite ABC Kit from Vector Laboratories, PK-7200), as recommended by the manufacturer, and nuclei were counterstained using Gill's hematoxylin.

TNX labelling was first assessed on human skin sections with different antibodies (sc-271594 (1/100) from Santa Cruz, AF6999 (1/100) from R&D Systems and two home-made antibodies provided by Joost SCHALKWIJK (1/100) and Manuel KOCH (1/1000)) (Supplementary Fig. S3), and sc-271,594 antibody (Santa Cruz, clone F11; 1/100) was then used to immunostain sections on two commercially available Tissue MicroArray (TMA) slides from US BioMax, Inc.: (1) *High-density multiple organ tumor and normal tissue array, including pathology grade, TNM and clinical stage*, 616 cases/616 cores (#MC6163) and (2) *Malignant mesothelioma with pleura tissue microarray, containing 4 cases of malignant mesothelioma, 2 pleura tissue* (#T392a). After TNX labelling, tissue cores were scanned using AxioScan.Z1 microscope (Zeiss). Each imaged spot was extracted by QuPath software (<https://qupath.github.io/>) and analyzed using Fiji software (<https://fiji.sc/>). Stromal and epithelial areas were separated thanks to Fiji Trainable Weka Segmentation plugin (https://imagej.net/Trainable_Weka_Segmentation). The segmentation training was newly performed for each tissue spot because of histological differences between the various analyzed organs and between tumoral and normal samples. Colors were then separated by “H DAB” Colour Deconvolution and DAB staining was quantified in stromal region (mean grey value). Reciprocal mean grey value (255 - mean grey value) was considered, as LookUp Table (LUT) is inverted in Fiji software. An example of the quantification process is shown in Supplementary Fig. S4. Tumoral and normal tissues were compared by non-parametric unpaired (Mann-Whitney) test. Additionally, TNX protein staining intensity was evaluated blindly by an anatomopathologist (Dr. Valérie HERVIEU, France).

Statistical analyses

All statistical analyses were performed using GraphPad Prism 7 software. Data were presented as mean \pm SEM. Groups were compared as explained in the previous sub-sections. p-Values < 0.05 were considered significant (**** $p < 0.0001$; *** $p < 0.001$; ** $p < 0.01$ and * $p < 0.05$). TCGA data statistics were calculated by the UALCAN web-portal.

Acknowledgments

We acknowledge the contribution of Federative Structure of Health Research Lyon-Est CNRS UMS3453/INSERM US7 and particularly Denis RESSNIKOFF from the microscopy platform (CIQLE) for his advice regarding TMA scanning and imaging analysis. Additionally, we greatly thank members of the histology and imaging facility

(PrImaTiss) at the LBTI institute for their advices regarding the setting for TNX immunodetection. We are very grateful to Manuel KOCH (University of Cologne, Germany) for kindly providing us the anti-human TNX antibodies used for antibody specificity validation. We also acknowledge Sylvie RICARD-BLUM for critical reading of the manuscript. SL and AA are recipients of PhD student fellowship from the French government (NMRT/ENS of Lyon). This work was supported by the “Ligue Nationale contre le Cancer, Comité du Rhône” and “Comité de l’Allier”, as well as by the “Fondation ARC pour la Recherche sur le Cancer” (PJA 20141201790).

CRedit author statement

Sophie Lot: Methodology, Data Curation, Software, Investigation, Formal Analysis, Visualization, Writing – Original draft; **Alexandre Aubert:** Validation; **Valérie Hervieu:** Formal Analysis, Investigation; **Naïma El Kholti:** Methodology; **Joost SCHALKWIJK:** Resources; **Bernard Verrier:** Funding acquisition; **Ulrich Valcourt:** Supervision, Writing – Review & Editing, Funding Acquisition; **Elise Lambert:** Conceptualization, Methodology, Visualization, Supervision, Writing – Original draft.

Appendix A. Supplementary data

Supplementary data to this article can be found online at <https://doi.org/10.1016/j.mbplus.2020.100021>.

Received 4 September 2019;

Received in revised form 12 December 2019;

Accepted 12 December 2019

Available online 20 January 2020

Keywords:

Tenascin-X;
Cancers;
mRNA and protein levels;
Prognosis marker;
Meta-analysis;
Tissue MicroArray

Abbreviations used:

CAF, Cancer-Associated Fibroblast; D.E.G., Differentially Expressed Genes; ECM, Extracellular Matrix; EDS, Ehlers-Danlos syndrome; FBG, fibrinogen; FNIII, fibronectin type III; GEO, Gene Expression Omnibus; GSE, GEO Series; HDAC1, histone deacetylase-1; lncRNA, long non-coding RNA; MMP, Matrix Metalloproteinase; MPNST, Malignant Peripheral Nerve Sheath Tumors; TCGA, The Cancer Genome Atlas; TMA, Tissue MicroArray; TME, Tumor MicroEnvironment; TN, Tenascin;

TNC, Tenascin-C; TNR, Tenascin-R; TNW, Tenascin-W; TNX, Tenascin-X; TSS, Transcription Start Site.

References

- [1] T. Rozario, D.W. DeSimone, The extracellular matrix in development and morphogenesis: a dynamic view, *Dev. Biol.* 341 (1) (May 2010) 126–140, <https://doi.org/10.1016/j.ydbio.2009.10.026>.
- [2] S.A. Wickström, K. Radovanac, R. Fässler, Genetic analyses of integrin signaling, *Cold Spring Harb. Perspect. Biol.* 3 (2) (Feb. 2011) <https://doi.org/10.1101/cshperspect.a005116>.
- [3] S.P. Hussain, C.C. Harris, Inflammation and cancer: an ancient link with novel potentials, *Int. J. Cancer* 121 (11) (2007) 2373–2380, <https://doi.org/10.1002/ijc.23173>.
- [4] G.M. Cooper, G.M. Cooper, *The Cell*, 2nd ed. Sinauer Associates, 2000.
- [5] H. Järveläinen, A. Sainio, M. Koulu, T.N. Wight, R. Penttinen, Extracellular matrix molecules: potential targets in pharmacotherapy, *Pharmacol. Rev.* 61 (2) (Jun. 2009) 198–223, <https://doi.org/10.1124/pr.109.001289>.
- [6] R.M. Bremnes, et al., The role of tumor stroma in cancer progression and prognosis: emphasis on carcinoma-associated fibroblasts and non-small cell lung cancer, *J. Thorac. Oncol. Off. Publ. Int. Assoc. Study Lung Cancer* 6 (1) (Jan. 2011) 209–217, <https://doi.org/10.1097/JTO.0b013e3181f8a1bd>.
- [7] D. Avery, P. Govindaraju, M. Jacob, L. Todd, J. Monslow, E. Puré, Extracellular matrix directs phenotypic heterogeneity of activated fibroblasts, *Matrix Biol.* 67 (2018) 90–106, <https://doi.org/10.1016/j.matbio.2017.12.003>.
- [8] S. Paget, The distribution of secondary growths in cancer of the breast. 1889, *Cancer Metastasis Rev.* 8 (2) (Aug. 1989) 98–101.
- [9] I.J. Fidler, The pathogenesis of cancer metastasis: the 'seed and soil' hypothesis revisited, *Nat. Rev. Cancer* 3 (6) (2003) 453–458, <https://doi.org/10.1038/nrc1098>.
- [10] M. Akhtar, A. Haider, S. Rashid, A.D.M.H. Al-Nabet, Paget's 'seed and soil' theory of cancer metastasis: an idea whose time has come, *Adv. Anat. Pathol.* 26 (1) (Jan. 2019) 69–74, <https://doi.org/10.1097/PAP.0000000000000219>.
- [11] G.S. Karagiannis, T. Poutahidis, S.E. Erdman, R. Kirsch, R. H. Riddell, E.P. Diamandis, Cancer-associated fibroblasts drive the progression of metastasis through both paracrine and mechanical pressure on cancer tissue, *Mol. Cancer Res.* MCR 10 (11) (Nov. 2012) 1403–1418, <https://doi.org/10.1158/1541-7786.MCR-12-0307>.
- [12] N.E. Sounni, A. Noel, Targeting the tumor microenvironment for cancer therapy, *Clin. Chem.* 59 (1) (Jan. 2013) 85–93, <https://doi.org/10.1373/clinchem.2012.185363>.
- [13] M.W. Pickup, J.K. Mouw, V.M. Weaver, The extracellular matrix modulates the hallmarks of cancer, *EMBO Rep.* 15 (12) (Dec. 2014) 1243–1253, <https://doi.org/10.15252/embr.201439246>.
- [14] X. Chen, E. Song, Turning foes to friends: targeting cancer-associated fibroblasts, *Nat. Rev. Drug Discov.* 18 (2) (Feb. 2019) 99–115, <https://doi.org/10.1038/s41573-018-0004-1>.
- [15] A.D. Theocharis, S.S. Skandalis, C. Gialeli, N.K. Karamanos, Extracellular matrix structure, *Adv. Drug Deliv. Rev.* 97 (Feb. 2016) 4–27, <https://doi.org/10.1016/j.addr.2015.11.001>.
- [16] N.K. Karamanos, A.D. Theocharis, T. Neill, R.V. Iozzo, Matrix modeling and remodeling: a biological interplay regulating tissue homeostasis and diseases, *Matrix Biol.* 75–76 (2019) 1–11, <https://doi.org/10.1016/j.matbio.2018.08.007>.
- [17] G. Botti, M. Cerrone, G. Scognamiglio, A. Anniciello, P.A. Ascierto, M. Cantile, Microenvironment and tumor progression of melanoma: new therapeutic perspectives, *J. Immunotoxicol.* 10 (3) (Sep. 2013) 235–252, <https://doi.org/10.3109/1547691X.2012.723767>.
- [18] T. Liu, L. Zhou, D. Li, T. Andl, Y. Zhang, Cancer-associated fibroblasts build and secure the tumor microenvironment, *Front. Cell Dev. Biol.* 7 (Apr. 2019) <https://doi.org/10.3389/fcell.2019.00060>.
- [19] R. Thakur, D.P. Mishra, Matrix reloaded: CCN, tenascin and SIBLING group of matricellular proteins in orchestrating cancer hallmark capabilities, *Pharmacol. Ther.* 168 (2016) 61–74, <https://doi.org/10.1016/j.pharmthera.2016.09.002>.
- [20] U. Valcourt, L.B. Alcaraz, J.-Y. Exposito, C. Lethias, L. Bartholin, Tenascin-X: beyond the architectural function, *Cell Adhes. Migr.* 9 (1–2) (Jan. 2015) 154–165, <https://doi.org/10.4161/19336918.2014.994893>.
- [21] R. Chiquet-Ehrismann, R.P. Tucker, Tenascins and the importance of adhesion modulation, *Cold Spring Harb. Perspect. Biol.* 3 (5) (May 2011) <https://doi.org/10.1101/cshperspect.a004960>.
- [22] R. Chiquet-Ehrismann, G. Orend, M. Chiquet, R.P. Tucker, K. S. Midwood, Tenascins in stem cell niches, *Matrix Biol.* 37 (Jul. 2014) 112–123, <https://doi.org/10.1016/j.matbio.2014.01.007>.
- [23] K.S. Midwood, M. Chiquet, R.P. Tucker, G. Orend, Tenascin-C at a glance, *J. Cell Sci.* 129 (23) (2016) 4321–4327, 01 <https://doi.org/10.1242/jcs.190546>.
- [24] Z. Sun, et al., Tenascin-C increases lung metastasis by impacting blood vessel invasions, *Matrix Biol.* 83 (Oct. 2019) 26–47, <https://doi.org/10.1016/j.matbio.2019.07.001>.
- [25] T. Murakami, et al., Tenascin C in colorectal cancer stroma is a predictive marker for liver metastasis and is a potent target of miR-198 as identified by microRNA analysis, *Br. J. Cancer* 117 (9) (Oct. 2017) 1360–1370, <https://doi.org/10.1038/bjc.2017.291>.
- [26] V. Gocheva, et al., Quantitative proteomics identify Tenascin-C as a promoter of lung cancer progression and contributor to a signature prognostic of patient survival, *Proc. Natl. Acad. Sci. U. S. A.* 114 (28) (2017) E5625–E5634, 11 <https://doi.org/10.1073/pnas.1707054114>.
- [27] W.-D. Ni, Z.-T. Yang, C.-A. Cui, Y. Cui, L.-Y. Fang, Y.-H. Xuan, Tenascin-C is a potential cancer-associated fibroblasts marker and predicts poor prognosis in prostate cancer, *Biochem. Biophys. Res. Commun.* 486 (3) (2017) 607–612, 06 <https://doi.org/10.1016/j.bbrc.2017.03.021>.
- [28] Z. Yang, W. Ni, C. Cui, L. Fang, Y. Xuan, Tenascin C is a prognostic determinant and potential cancer-associated fibroblasts marker for breast ductal carcinoma, *Exp. Mol. Pathol.* 102 (2) (2017) 262–267, <https://doi.org/10.1016/j.yexmp.2017.02.012>.
- [29] C.M. Lowy, T. Oskarsson, Tenascin C in metastasis: a view from the invasive front, *Cell Adhes. Migr.* 9 (1–2) (2015) 112–124, <https://doi.org/10.1080/19336918.2015.1008331>.
- [30] C. Shen, et al., Tenascin-C expression is significantly associated with the progression and prognosis in gastric GISTs, *Medicine (Baltimore)* 98 (2) (Jan. 2019) <https://doi.org/10.1097/MD.00000000000014045>.
- [31] R.P. Tucker, M. Degen, The expression and possible functions of Tenascin-W during development and disease,

- Front. Cell Dev. Biol. 7 (Apr. 2019) <https://doi.org/10.3389/fcell.2019.00053>.
- [32] M. Degen, et al., Tenascin-W is a novel marker for activated tumor stroma in low-grade human breast cancer and influences cell behavior, *Cancer Res.* 67 (19) (Oct. 2007) 9169–9179, <https://doi.org/10.1158/0008-5472.CAN-07-0666>.
- [33] M. Degen, et al., Tenascin-W, a new marker of cancer stroma, is elevated in sera of colon and breast cancer patients, *Int. J. Cancer* 122 (11) (Jun. 2008) 2454–2461, <https://doi.org/10.1002/ijc.23417>.
- [34] E. Martina, et al., Tenascin-W is a specific marker of glioma-associated blood vessels and stimulates angiogenesis in vitro, *FASEB J. Off. Publ. Fed. Am. Soc. Exp. Biol.* 24 (3) (Mar. 2010) 778–787, <https://doi.org/10.1096/fj.09-140491>.
- [35] F. Brellier, et al., The adhesion modulating properties of tenascin-W, *Int. J. Biol. Sci.* 8 (2) (2012) 187–194.
- [36] L.B. Derr, L.A. McKae, R.P. Tucker, The distribution of tenascin-R in the developing avian nervous system, *J. Exp. Zool.* 280 (2) (Feb. 1998) 152–164.
- [37] B. Fuss, E.S. Wintergerst, U. Bartsch, M. Schachner, Molecular characterization and in situ mRNA localization of the neural recognition molecule J1-160/180: a modular structure similar to tenascin, *J. Cell Biol.* 120 (5) (Mar. 1993) 1237–1249, <https://doi.org/10.1083/jcb.120.5.1237>.
- [38] P. Pesheva, S. Gloor, M. Schachner, R. Probstmeier, Tenascin-R is an intrinsic autocrine factor for oligodendrocyte differentiation and promotes cell adhesion by a sulfate-mediated mechanism, *J. Neurosci.* 17 (12) (Jun. 1997) 4642–4651.
- [39] R. Probstmeier, J. Nellen, S. Gloor, A. Wernig, P. Pesheva, Tenascin-R is expressed by Schwann cells in the peripheral nervous system, *J. Neurosci. Res.* 64 (1) (Apr. 2001) 70–78, <https://doi.org/10.1002/jnr.1055>.
- [40] F. Chiovaro, R. Chiquet-Ehrismann, M. Chiquet, Transcriptional regulation of tenascin genes, *Cell Adhes. Migr.* 9 (1–2) (2015) 34–47, <https://doi.org/10.1080/19336918.2015.1008333>.
- [41] B. Anlar, A. Gunel-Ozcan, Tenascin-R: role in the central nervous system, *Int. J. Biochem. Cell Biol.* 44 (9) (Sep. 2012) 1385–1389, <https://doi.org/10.1016/j.biocel.2012.05.009>.
- [42] I. El Ayachi, C. Fernandez, N. Baeza, A.M. De Paula, P. Pesheva, D. Figarella-Branger, Spatiotemporal distribution of tenascin-R in the developing human cerebral cortex parallels neuronal migration, *J. Comp. Neurol.* 519 (12) (Aug. 2011) 2379–2389, <https://doi.org/10.1002/cne.22632>.
- [43] J. Bristow, M.K. Tee, S.E. Gitelman, S.H. Mellon, W.L. Miller, Tenascin-X: a novel extracellular matrix protein encoded by the human XB gene overlapping P450c21B, *J. Cell Biol.* 122 (1) (Jul. 1993) 265–278.
- [44] G.H. Burch, M.A. Bedolli, S. McDonough, S.M. Rosenthal, J. Bristow, Embryonic expression of tenascin-X suggests a role in limb, muscle, and heart development, *Dev. Dyn. Off. Publ. Am. Assoc. Anat.* 203 (4) (Aug. 1995) 491–504, <https://doi.org/10.1002/aja.1002030411>.
- [45] C. Lethias, A. Carisey, J. Comte, C. Cluzel, J.-Y. Exposito, A model of tenascin-X integration within the collagenous network, *FEBS Lett.* 580 (26) (Oct. 2006) 6281–6285, <https://doi.org/10.1016/j.febslet.2006.10.037>.
- [46] T. Sakai, et al., Tenascin-X expression in tumor cells and fibroblasts: glucocorticoids as negative regulators in fibroblasts, *J. Cell Sci.* 109 (Pt 8) (Aug. 1996) 2069–2077.
- [47] K. Hasegawa, T. Yoshida, K. Matsumoto, K. Katsuta, S. Waga, T. Sakakura, Differential expression of tenascin-C and tenascin-X in human astrocytomas, *Acta Neuropathol. (Berl.)* 93 (5) (May 1997) 431–437.
- [48] P. Lévy, et al., Microarray-based identification of tenascin C and tenascin XB, genes possibly involved in tumorigenesis associated with neurofibromatosis type 1, *Clin. Cancer Res. Off. J. Am. Assoc. Cancer Res.* 13 (2 Pt 1) (Jan. 2007) 398–407, <https://doi.org/10.1158/1078-0432.CCR-06-0182>.
- [49] C. Geffrotin, et al., Opposite regulation of tenascin-C and tenascin-X in MeLiM swine heritable cutaneous malignant melanoma, *Biochim. Biophys. Acta* 1524 (2–3) (Dec. 2000) 196–202.
- [50] S.O. Lee, S.Y. Lee, S.R. Lee, W. Ju, S.C. Kim, Tenascin-X and leukemia inhibitory factor receptor are down-regulated in leiomyoma compared with normal myometrium, *J. Gynecol. Oncol.* 19 (2) (Jun. 2008) 139–144, <https://doi.org/10.3802/jgo.2008.19.2.139>.
- [51] B. Davidson, et al., Gene expression signatures differentiate ovarian/peritoneal serous carcinoma from diffuse malignant peritoneal mesothelioma, *Clin. Cancer Res.* 12 (20) (Oct. 2006) 5944–5950, <https://doi.org/10.1158/1078-0432.CCR-06-1059>.
- [52] Y. Yuan, et al., Tenascin-X is a novel diagnostic marker of malignant mesothelioma, *Am. J. Surg. Pathol.* 33 (11) (Nov. 2009) 1673–1682, <https://doi.org/10.1097/PAS.0b013e3181b6bde3>.
- [53] K. Nakayama, et al., Tenascin XB is a novel diagnostic marker for malignant mesothelioma, *Anticancer Res.* 39 (2) (Feb. 2019) 627–633, <https://doi.org/10.21873/anticancer.13156>.
- [54] M. Kramer, S. Pierredon, P. Ribaux, J.-C. Tille, P. Petignat, M. Cohen, Secretome identifies Tenascin-X as a potent marker of ovarian cancer, *Biomed. Res. Int.* 2015 (2015) 208017, <https://doi.org/10.1155/2015/208017>.
- [55] D.S. Chandrashekar, et al., UALCAN: a portal for facilitating tumor subgroup gene expression and survival analyses, *Neoplasia N. Y. N* 19 (8) (Aug. 2017) 649–658, <https://doi.org/10.1016/j.neo.2017.05.002>.
- [56] Y.P. Yu, et al., Gene expression alterations in prostate cancer predicting tumor aggression and preceding development of malignancy, *J. Clin. Oncol. Off. J. Am. Soc. Clin. Oncol.* 22 (14) (Jul. 2004) 2790–2799, <https://doi.org/10.1200/JCO.2004.05.158>.
- [57] J. Schalkwijk, et al., A recessive form of the Ehlers-Danlos syndrome caused by tenascin-X deficiency, *N. Engl. J. Med.* 345 (16) (Oct. 2001) 1167–1175, <https://doi.org/10.1056/NEJMoa002939>.
- [58] E. Gobin, et al., A pan-cancer perspective of matrix metalloproteases (MMP) gene expression profile and their diagnostic/prognostic potential, *BMC Cancer* 19 (1) (Jun. 2019), 581. <https://doi.org/10.1186/s12885-019-5768-0>.
- [59] A. Chakravarthy, L. Khan, N.P. Bensler, P. Bose, D.D.D. Carvalho, TGF- β -associated extracellular matrix genes link cancer-associated fibroblasts to immune evasion and immunotherapy failure, *Nat. Commun.* 9 (1) (Nov. 2018) 1–10, <https://doi.org/10.1038/s41467-018-06654-8>.
- [60] Cancer Genome Atlas Research Network, The molecular taxonomy of primary prostate cancer, *Cell* 163 (4) (Nov. 2015) 1011–1025, <https://doi.org/10.1016/j.cell.2015.10.025>.
- [61] K.K. Huang, et al., Genomic and epigenomic profiling of high-risk intestinal metaplasia reveals molecular determinants of progression to gastric cancer, *Cancer Cell* 33 (1) (2018) 137–150.e508. [10.1016/j.ccell.2017.11.018](https://doi.org/10.1016/j.ccell.2017.11.018).
- [62] V.R. Krishnaswamy, A. Benbenishty, P. Blinder, I. Sagi, Demystifying the extracellular matrix and its proteolytic remodeling in the brain: structural and functional insights,

- Cell. Mol. Life Sci. CMLS 76 (16) (Aug. 2019) 3229–3248, <https://doi.org/10.1007/s00018-019-03182-6>.
- [63] M. Koshiyama, N. Matsumura, I. Konishi, Subtypes of ovarian cancer and ovarian cancer screening, *Diagn. Basel Switz.* 7 (1) (Mar. 2017) <https://doi.org/10.3390/diagnostics7010012>.
- [64] S. Lheureux, C. Gourley, I. Vergote, A.M. Oza, Epithelial ovarian cancer, *Lancet Lond. Engl.* 393 (10177) (Mar. 2019) 1240–1253, [https://doi.org/10.1016/S0140-6736\(18\)32552-2](https://doi.org/10.1016/S0140-6736(18)32552-2).
- [65] M. Ekblom, R. Fässler, B. Tomasini-Johansson, K. Nilsson, P. Ekblom, Downregulation of tenascin expression by glucocorticoids in bone marrow stromal cells and in fibroblasts, *J. Cell Biol.* 123 (4) (Nov. 1993) 1037–1045, <https://doi.org/10.1083/jcb.123.4.1037>.
- [66] M. Speek, F. Barry, W.L. Miller, Alternate promoters and alternate splicing of human tenascin-X, a gene with 5' and 3' ends buried in other genes, *Hum. Mol. Genet.* 5 (11) (Nov. 1996) 1749–1758.
- [67] S.D. Wijesuriya, J. Bristow, W.L. Miller, Localization and analysis of the principal promoter for human tenascin-X, *Genomics* 80 (4) (Oct. 2002) 443–452.
- [68] A. Kato, T. Endo, S. Abiko, H. Ariga, K. Matsumoto, Induction of truncated form of tenascin-X (XB-S) through dissociation of HDAC1 from SP-1/HDAC1 complex in response to hypoxic conditions, *Exp. Cell Res.* 314 (14) (Aug. 2008) 2661–2673, <https://doi.org/10.1016/j.yexcr.2008.05.019>.
- [69] T. Endo, H. Ariga, K. Matsumoto, Truncated form of tenascin-X, XB-S, interacts with mitotic motor kinesin Eg5, *Mol. Cell. Biochem.* 320 (1–2) (Jan. 2009) 53–66, <https://doi.org/10.1007/s11010-008-9898-y>.
- [70] M. Smolle, S. Uranitsch, A. Gerger, M. Pichler, J. Haybaeck, Current status of long non-coding RNAs in human cancer with specific focus on colorectal cancer, *Int. J. Mol. Sci.* 15 (8) (Aug. 2014) 13993–14013, <https://doi.org/10.3390/ijms150813993>.
- [71] M. Seles, et al., Current insights into long non-coding RNAs in renal cell carcinoma, *Int. J. Mol. Sci.* 17 (4) (Apr. 2016) 573, <https://doi.org/10.3390/ijms17040573>.
- [72] S. Cerk, et al., Current status of long non-coding RNAs in human breast cancer, *Int. J. Mol. Sci.* 17 (9) (Sep. 2016) <https://doi.org/10.3390/ijms17091485>.
- [73] S.-P. Yan, et al., LncRNA LINC01305 silencing inhibits cell epithelial-mesenchymal transition in cervical cancer by inhibiting TNXB-mediated PI3K/Akt signalling pathway, *J. Cell. Mol. Med.* 23 (4) (Apr. 2019) 2656–2666, <https://doi.org/10.1111/jcmm.14161>.
- [74] K. Matsumoto, et al., Tumour invasion and metastasis are promoted in mice deficient in tenascin-X, *Genes Cells Devoted Mol. Cell. Mech.* 6 (12) (Dec. 2001) 1101–1111.
- [75] K.-I. Matsumoto, K. Takahashi, A. Yoshiki, M. Kusakabe, H. Ariga, Invasion of melanoma in double knockout mice lacking tenascin-X and tenascin-C, *Jpn. J. Cancer Res. Gann* 93 (9) (Sep. 2002) 968–975.
- [76] T. Minamitani, H. Ariga, K. Matsumoto, Adhesive defect in extracellular matrix Tenascin-X-null fibroblasts: a possible mechanism of tumor invasion, *Biol. Pharm. Bull.* 25 (11) (2002) 1472–1475, <https://doi.org/10.1248/bpb.25.1472>.